Infrared Photodissociation Spectroscopy of Protonated Formic Acid−Water Binary Clusters, $H^+\cdot(HCOOH)_n\cdot H_2O$ ($n = 1-5$). Spectroscopic Study of Ion Core Switch Model and Magic Number

Yoshiya Inokuchi and Nobuyuki Nishi*

Institute for Molecular Science, Myodaiji, Okazaki 444-8585, Japan

Received: December 5, 2001; In Final Form: February 21, 2002

Infrared spectra of protonated formic acid−water binary clusters, $H^+\cdot(HCOOH)_n\cdot H_2O$ ($n = 1-5$), are investigated by infrared photodissociation spectroscopy and ab initio molecular orbital calculations. The asymmetric OH stretching vibration of water is observed in the infrared photodissociation spectra of the clusters with $n = 1-3$; it disappears in the spectra of the $n = 4$ and 5 clusters. On detailed comparison of the observed infrared spectra with calculated ones, the most stable geometric structures are obtained for the $n = 1-5$ clusters. These results suggest that the clusters switch the ion cores from $HCOOH_2^+$ for $n = 1-3$ to H_3O^+ for $n = 4$ and 5. The $n = 5$ cluster has a cyclic-type structure; the H_3O^+ ion core is fully surrounded and stabilized by five formic acid molecules. This characteristic nature produces a magic number of the $n = 5$ cluster.

1. Introduction

Mass-selected photodissociation spectroscopy is one of the most useful techniques for investigating cluster ions.[1−5] In particular, infrared photodissociation spectroscopy is a fruitful probe into the geometric structures. For clusters containing OH or NH groups, the stretching frequencies of these groups are very sensitive to the hydrogen-bonding formation. By measuring infrared photodissociation spectra, one can obtain the frequencies and discuss the cluster structures.

Carboxylic acid (RCOOH) is one of the popular acids in organic chemistry. Because a carboxylic acid molecule has a few groups capable of the hydrogen-bonding formation, its aggregates may show various kinds of intermolecular interaction.[6] In the crystals, carboxylic acid molecules are interlinked to form either a cyclic dimer or an infinite chain; the linkage manner depends on the substituent R.[7] Formic acid, HCOOH, is the simplest carboxylic acid. Formic acid molecules form an infinite chain in the crystal[7] and a cyclic dimer in the gas phase.[8] Lifshitz and co-workers actively investigated protonated formic acid clusters, $H^+\cdot(HCOOH)_n$, and their aqueous clusters, $H^+\cdot(HCOOH)_n\cdot(H_2O)_m$.[9−11] In the mass spectrum of formic acid−water binary clusters, the $H^+\cdot(HCOOH)_5\cdot H_2O$ ion is observed particularly to be abundant; this cluster size is called a magic number. Collisionally activated dissociations (CAD) of $H^+\cdot(HCOOH)_n\cdot H_2O$ result in a water loss for smaller n and a formic acid loss for larger n. According to the CAD result, they suggested a "proton switch" model; there is a critical cluster size, below which an $HCOOH_2^+$ ion core is more stable than H_3O^+ and above which an H_3O^+ ion core is preferential. However, the critical cluster size was unspecified precisely, because the threshold of change in the branching ratio is not so sharp. Lifshitz and co-workers also studied semiempirical and ab initio molecular orbital (MO) calculations of $H^+\cdot(HCOOH)_n\cdot H_2O$ ($n = 1-8$).[11] On the basis of the total energies of several stable isomers, they concluded that the proton switch occurs between $n = 3$ and 4. Their ab initio calculations were done at the HF/4-31G# level. In this basis set, polarization functions are applied not to positively charged carbon atoms but to negatively charged oxygen atoms. They mentioned that higher level calculations should be necessary to confirm the experimentally detected magic number, $H^+\cdot(HCOOH)_5\cdot H_2O$.

In this paper, we report an experimental and a theoretical investigation of the structures of $H^+\cdot(HCOOH)_n\cdot H_2O$ ($n = 1-5$). Infrared photodissociation spectra of the clusters were measured by use of an ion guide spectrometer and a pulsed infrared laser. Optimized structures and theoretical infrared spectra were obtained by ab initio MO calculations. The cluster structures, the ion core switch model, and the magic number are discussed by comparison of the observed infrared spectra with the calculated ones.

2. Experimental and Computational Details

The infrared photodissociation spectra of $H^+\cdot(HCOOH)_n\cdot H_2O$ ($n = 1-5$) were measured by use of the ion guide spectrometer with two quadrupole mass filters.[12,13] A gas mixture of formic acid, water, and argon was introduced into a vacuum chamber through a pulsed nozzle (General Valve series 9) with a 0.80 mm orifice diameter and a 300 μs pulse duration. The total stagnation pressure was 2×10^5 Pa. Neutral formic acid−water binary clusters were ionized by an electron-impact ionizer situated near the exit of the pulsed nozzle. The electron kinetic energy was adjusted to 350 eV. After passing through a skimmer, produced cluster ions were introduced into the spectrometer. Parent ions were isolated by the first quadrupole mass filter. After the deflection by 90° through an ion bender, the parent ions were led into a quadrupole ion guide. The ion beam was merged with a laser beam in the ion guide, and the parent ions were excited into vibrationally excited states. The excitation induces fragmentation of the parent ions. Resultant fragment ions were mass-analyzed by the second quadrupole mass filter and detected by a secondary electron multiplier tube (Murata Ceratron EMS-6081B). For the normalization of the

* To whom correspondence should be addressed. E-mail: nishi@ims.ac.jp.

10.1021/jp014432n CCC: $22.00
Published on Web 04/18/2002

fragment−ion yield, the power of the dissociation laser was monitored by a pyroelectric detector (Molectron P1-15H-CC). Both the ion and the laser signals were fed into a digital storage oscilloscope (LeCroy 9314A). The oscilloscope was controlled by a microcomputer through a GPIB interface. One can obtain photodissociation spectra of parent ions by plotting the normalized yields of the fragment ions against the wavenumbers of the dissociation laser.

A tunable infrared source was an optical parametric oscillator (OPO) system (Continuum Mirage 3000) pumped with an injection-seeded Nd:YAG laser (Continuum Powerlite 9010). The output energy used in this work was 1−2 mJ/pulse. The line width was approximately 1 cm^{-1}. The wavenumber of the infrared laser was calibrated by a commercial wavemeter (Burleigh WA-4500).

Moreover, the $H^+ \cdot (HCOOH)_n \cdot H_2O$ clusters were analyzed by ab initio MO calculations. The calculations were made by the SGI2800 computer of Okazaki National Research Institutes with the Gaussian 98 program package.[14] Geometry optimization and vibrational frequency evaluation were done on the basis of the density functional theory in which Becke's three-parameter hybrid functionals are combined with the Lee−Yang−Parr correlation functional (B3LYP). The Pople's 6-31++G(d,p) basis set was used for all of the calculations.

3. Results

Figure 1a shows a mass spectrum of protonated formic acid−water binary clusters, $H^+ \cdot (HCOOH)_n \cdot (H_2O)_m$. We abbreviate $H^+ \cdot (HCOOH)_n \cdot (H_2O)_m$ to (n,m). The main peaks are attributed to protonated formic acid clusters, $(n,0)$, with $n = 1-6$. Protonated formic acid clusters with one water molecule, $(n,1)$, also appear in the spectrum. Figure 1b depicts the ion intensities of $(n,1)$ relative to those of $(n,0)$, $[(n,1)]/[(n,0)]$, for $n = 1-7$. Apparently, the ion intensity becomes higher and higher with increasing cluster size, n, and the intensity of the (5,1) cluster is much higher than those of other $(n,1)$ clusters. This result indicates that the $(n,1)$ clusters tend to fold the water molecule more tightly and tightly with increasing cluster size and that the (5,1) cluster has a particularly stable structure.

Figure 2a illustrates photofragment ion mass spectra of $H^+ \cdot (HCOOH)_n \cdot H_2O$ ($n = 1-6$). The parent ions were irradiated by the infrared light with a wavenumber of 3550 cm^{-1}. The resultant fragment ions were mass-analyzed by the second quadrupole mass filter. The abscissa represents the mass number relative to the parent ions; signals at −18 mass number signify that the evaporation of one water molecule (H_2O loss) occurs after the infrared excitation. Similarly, signals at −46 mass number mean the evaporation of one formic acid molecule (HCOOH loss). Figure 2b shows the photodissociation branching ratio as a function of cluster size. This figure is produced from the result in Figure 2a. The H_2O loss channel is prominent for $n = 1-3$. For $n = 4$, the branching ratio of the HCOOH loss channel becomes comparable to that of the H_2O loss channel. For $n = 5$ and 6, the branching ratio of the HCOOH channel is larger than that of the H_2O channel.

Infrared photodissociation spectra of $H^+ \cdot (HCOOH)_n \cdot H_2O$ ($n = 1-5$) are presented in Figure 3. These spectra were measured by monitoring the yields of the H_2O loss channel ($n = 1-3$) or the HCOOH loss channel ($n = 4$ and 5). One or a few bands with relatively narrow bandwidths are observed in the 3400−3800 cm^{-1} region for $n = 1-4$. The band positions are 3490 and 3570 cm^{-1} for $n = 1$, 3540 and 3605 cm^{-1} for $n = 2$, 3552, 3615, and 3645 cm^{-1} for $n = 3$, and 3555 cm^{-1} for $n = 4$. In the spectra of $n = 3-5$, broader bands are also observed in the 3000−3400 cm^{-1} region.

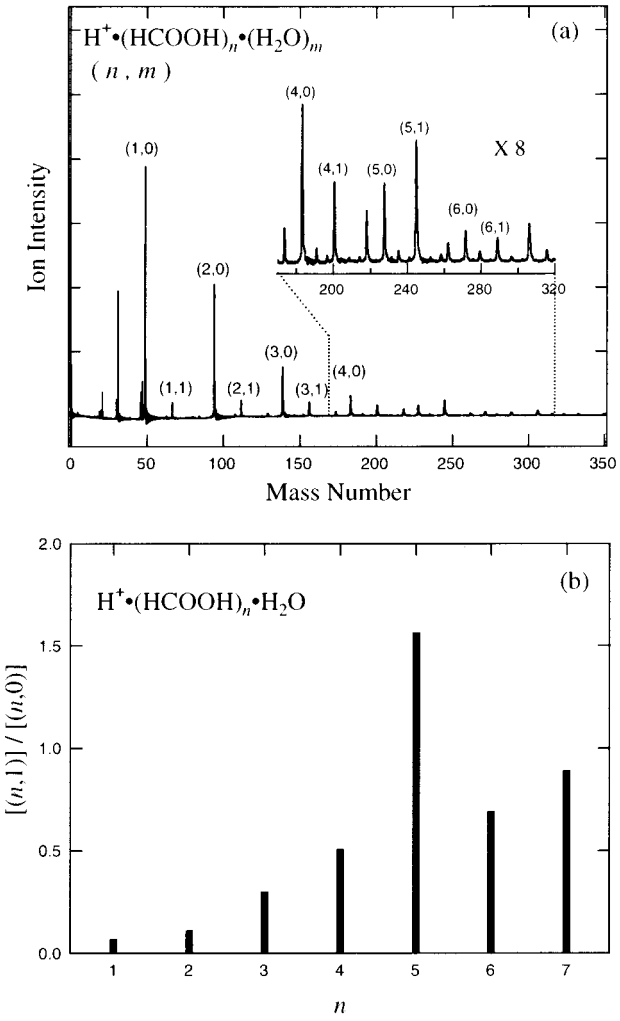

Figure 1. (a) Mass spectrum of protonated formic acid−water binary clusters, $H^+ \cdot (HCOOH)_n \cdot (H_2O)_m$. (b) Observed ion intensities of $(n,1)$ relative to $(n,0)$ for $n = 1-7$.

Figure 4 shows stable isomers of $H^+ \cdot (HCOOH)_n \cdot H_2O$ ($n = 1-5$) obtained by ab initio MO calculations. Table 1 summarizes difference in total energies and ion core species of the isomers. We confirmed the potential minima by checking that all of the vibrational frequencies are real. In Figure 4, the most stable isomers are arranged on the left side. All of the stable isomers obtained in this study are essentially the same as those obtained by Lifshitz and co-workers.[11] Structure I represents the most stable form of $n = 1$. The proton that links two molecules together is located closer to the formic acid molecule. This result agrees with the expectation based on the proton affinities of formic acid (177.3 kcal/mol) and water (165 kcal/mol).[15] For $n = 2$, the most stable isomer is structure II. The proton is attached to one formic acid molecule and forms an $HCOOH_2^+$ ion core. The ion core is solvated by the other formic acid molecule and a water molecule. Structure III is also stable in our calculations; the ion core is an H_3O^+ ion, and two formic acid molecules are bound to the ion core. For $n = 3$, the most stable isomer has a chain form (structure IV); the ion core is an $HCOOH_2^+$ ion, and a water molecule is at the periphery of the cluster chain. There is another stable structure with an H_3O^+ ion core (structure V). The ion core is solvated by three formic acid molecules. For $n = 4$, structure VI is the most stable isomer. An H_3O^+ ion core is directly solvated by three formic acid molecules. Structure VII has the chain form; the ion core is

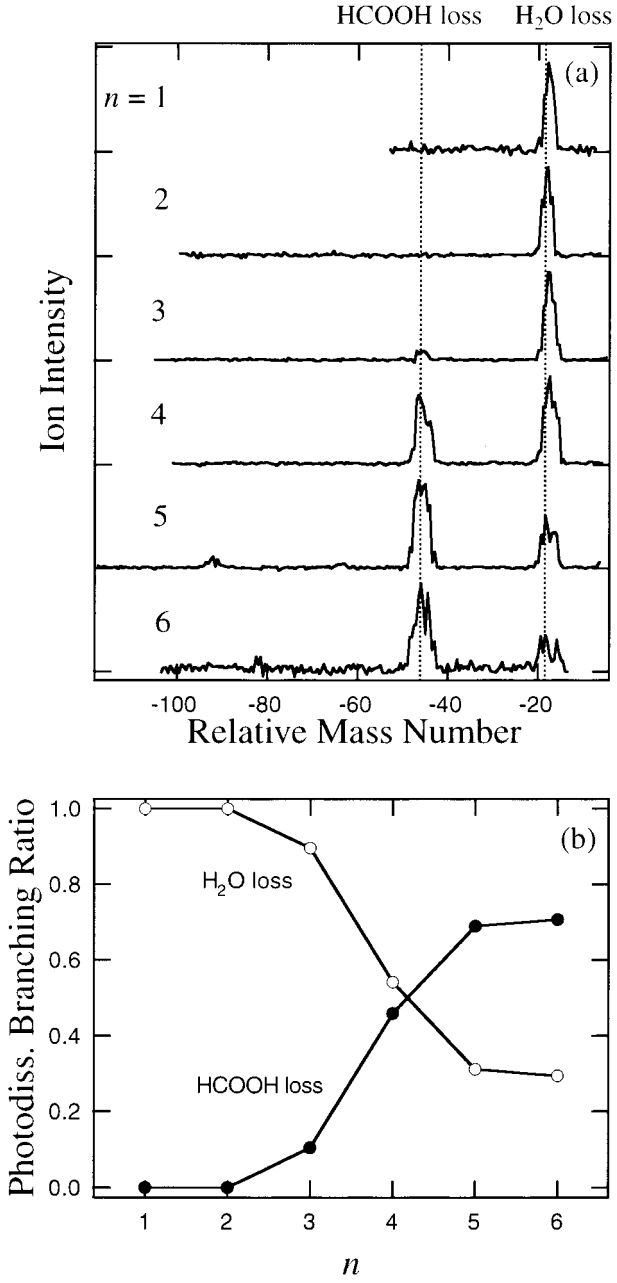

Figure 2. (a) Photofragment ion mass spectra for $H^+\cdot(HCOOH)_n\cdot H_2O$ ($n = 1-6$) dissociated at 3550 cm^{-1}. The abscissa represents the mass number relative to the respective parent ions. (b) Photodissociation branching ratio for $H^+\cdot(HCOOH)_n\cdot H_2O$ ($n = 1-6$) at 3550 cm^{-1}.

$HCOOH_2^+$, and a water molecule is bound to the end of the chain. The most stable structure of $n = 5$ (structure VIII) has an H_3O^+ ion core. Five formic acid molecules surround the ion core and form a ring. Structure IX exhibits an interesting structure; an H_2O molecule is at one end of the cluster chain, and a cyclic dimer is located at another end of the chain. Lifshitz and co-workers have previously demonstrated the occurrence of the cyclic dimer in theoretical calculations[11] and experimental observations of dimer evaporations.[9]

Calculated infrared spectra are displayed with the observed ones in Figures 5−9. The bar spectra labeled by the numbers I−IX correspond to the calculated spectra of structures I−IX, respectively. Tables 2 and 3 summarize the vibrational frequencies, the infrared intensities, and the assignments for $H^+\cdot(HCOOH)_n\cdot H_2O$ ($n = 1-5$). We use a scaling factor of 0.9345 for the calculated vibrational frequencies. Comparison of the observed spectra with the calculated ones is discussed in the next section.

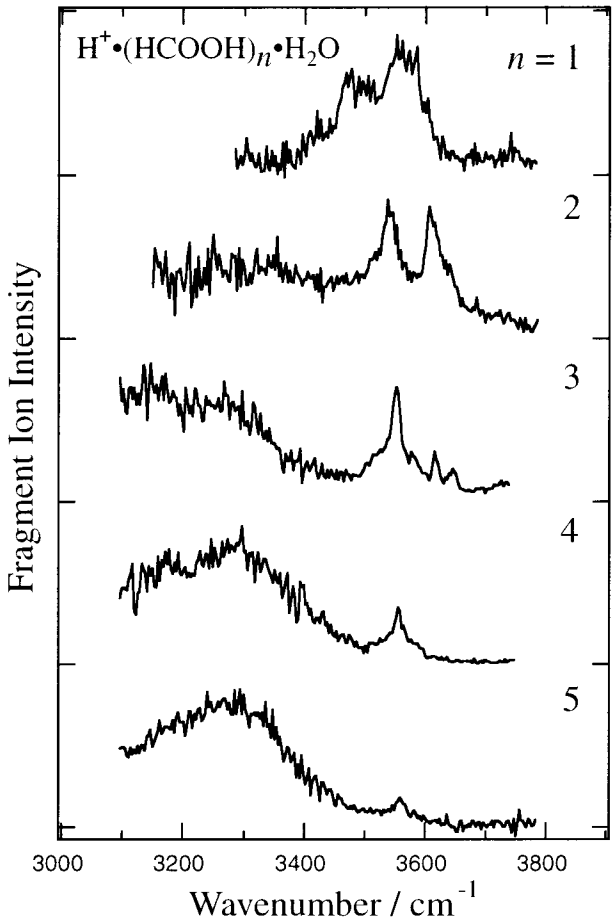

Figure 3. Infrared photodissociation spectra of $H^+\cdot(HCOOH)_n\cdot H_2O$ ($n = 1-5$) in the 3100−3800 cm^{-1} region. These spectra were measured by monitoring the yields of the fragment $H^+\cdot(HCOOH)_n$ ion (H_2O loss channel) for $n = 1-3$ or the $H^+\cdot(HCOOH)_{n-1}\cdot H_2O$ ion (HCOOH loss channel) for $n = 4$ and 5. For the $n = 3-5$ clusters, essentially the same spectra were obtained by monitoring the counterpart of the respective fragments.

4. Discussion

As shown in Figure 1b, the relative ion intensity of the $H^+\cdot(HCOOH)_n\cdot H_2O$ clusters increases with increasing n, and the $H^+\cdot(HCOOH)_5\cdot H_2O$ cluster is the most abundant. This result indicates that the water molecule is bound to the clusters more tightly with increasing n and that the $H^+\cdot(HCOOH)_5\cdot H_2O$ cluster has a particularly stable structure. In Figure 2, one can see that vibrationally excited $H^+\cdot(HCOOH)_n\cdot H_2O$ clusters evaporate mainly one water molecule for smaller n and one formic acid molecule for larger n. This result compels the same suggestion that the $H^+\cdot(HCOOH)_n\cdot H_2O$ clusters hold the water molecule more tightly with increasing n. A drastic change in the photodissociation branching is seen at $n = 4$; the ratio of the HCOOH loss channel becomes comparable with that of the H_2O loss channel at $n = 4$. This feature implies some structural change of the clusters between $n = 1-3$ and $n = 4$ and 5.

The theoretical calculations show the same tendency. For $n = 1-3$, the most stable isomers have the chain form; the water molecule is at the periphery of the chain. For $n = 4$ and 5, however, the most stable isomers are the cyclic form; the H_3O^+ ion exists in the clusters, and the formic acid molecules

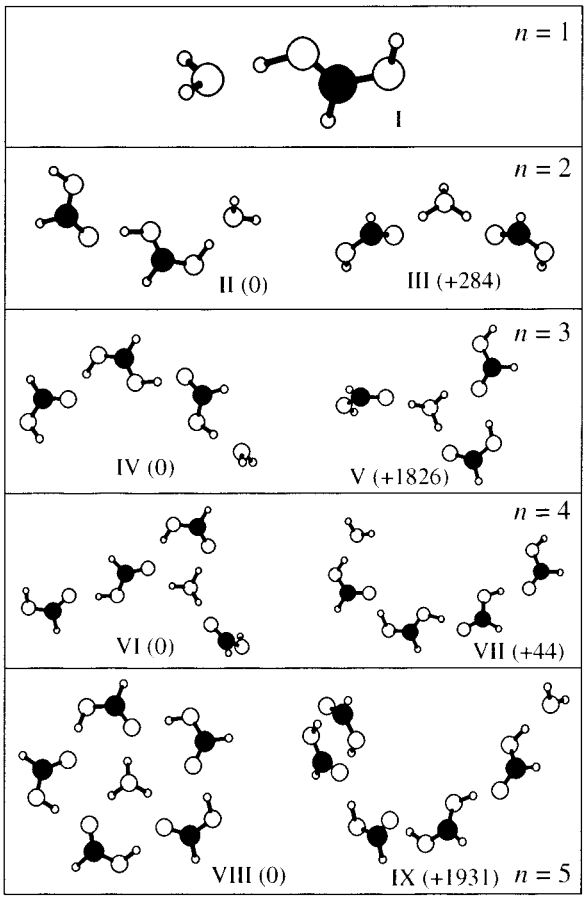

Figure 4. Optimized structures of $H^+ \cdot (HCOOH)_n \cdot H_2O$ for $n = 1$ (I), 2 (II and III), 3 (IV and V), 4 (VI and VII), and 5 (VIII and IX). These structures were calculated at the B3LYP/6-31++G(d,p) level. The numbers in the parentheses are the energies relative to those of the most stable isomers in cm^{-1}.

TABLE 1: B3LYP/6-31++G(d,p) Calculation of Difference in Total Energies (ΔE) and Ion Core Species of $H^+ \cdot (HCOOH)_n \cdot H_2O$ ($n = 1-5$)

n		$\Delta E^a/cm^{-1}$	ion core	n		$\Delta E^a/cm^{-1}$	ion core
1	I		$HCOOH_2^+$	4	VI	0	H_3O^+
2	II	0	$HCOOH_2^+$		VII	44	$HCOOH_2^+$
	III	284	H_3O^+	5	VIII	0	H_3O^+
3	IV	0	$HCOOH_2^+$		IX	1931	$HCOOH_2^+$
	V	1826	H_3O^+				

[a] Difference in total energy relative to those of the most stable isomers.

stabilizethe H_3O^+ ion core by surrounding it. The ion core switch from $HCOOH_2^+$ to H_3O^+ may occur between $n = 3$ and 4. This theoretical result agrees with the experimental suggestion described in the previous paragraph.

Prior to the detailed comparison of the observed infrared spectra with the calculated ones, let us summarize information on the infrared spectra of formic acid and water. The OH stretching band of the formic acid monomer appears at 3550.5 cm^{-1} in the infrared spectrum.[16] The infrared spectrum of water in the gas phase exhibits two bands at 3657 and 3756 cm^{-1}.[17] These bands are attributed to the symmetric and the asymmetric OH stretching vibrations, respectively. In the sequel, the words "HCOOH" and "H_2O" are used to represent the formic acid and the water molecule being at the periphery of the clusters, for assignments of the free OH stretching bands. The assignments of the free OH stretching vibrations are supposed to be understood from the cluster structures shown in Figure 4.

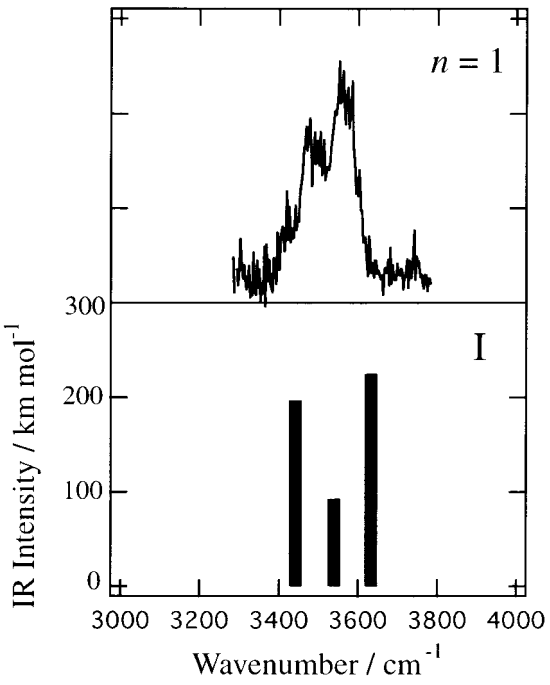

Figure 5. Comparison of the infrared photodissociation spectrum with the calculated infrared spectrum for $n = 1$. The Roman number, I, corresponds to structure I shown in Figure 4.

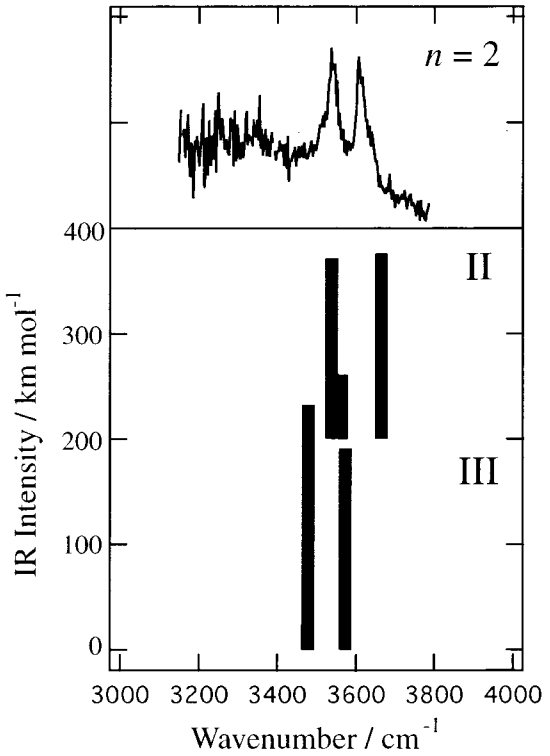

Figure 6. Comparison of the infrared photodissociation spectrum with the calculated infrared spectra for $n = 2$.

Figure 5 shows the observed infrared spectrum and the calculated one for $n = 1$. In the observed spectrum, two maxima appear at 3490 and 3570 cm^{-1}. In the calculated spectrum of structure I, a free OH stretching vibration of $HCOOH_2^+$ appears at 3442 cm^{-1}; a symmetric and an asymmetric OH stretching vibration of H_2O are seen at 3539 and 3632 cm^{-1}, respectively. On the basis of an intensity resemblance between the two spectra, the calculated three bands may overlap in the observed spectrum; the observed bands at 3490 and 3570 cm^{-1} are

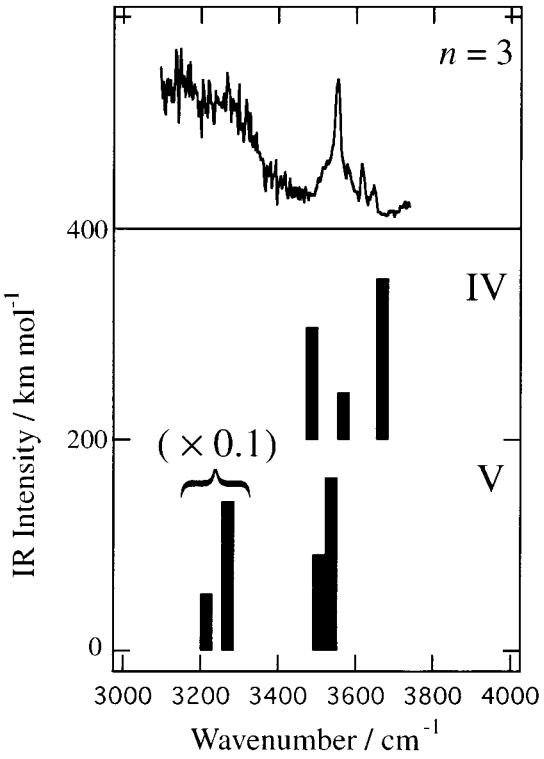

Figure 7. Comparison of the infrared photodissociation spectrum with the calculated infrared spectra for $n = 3$.

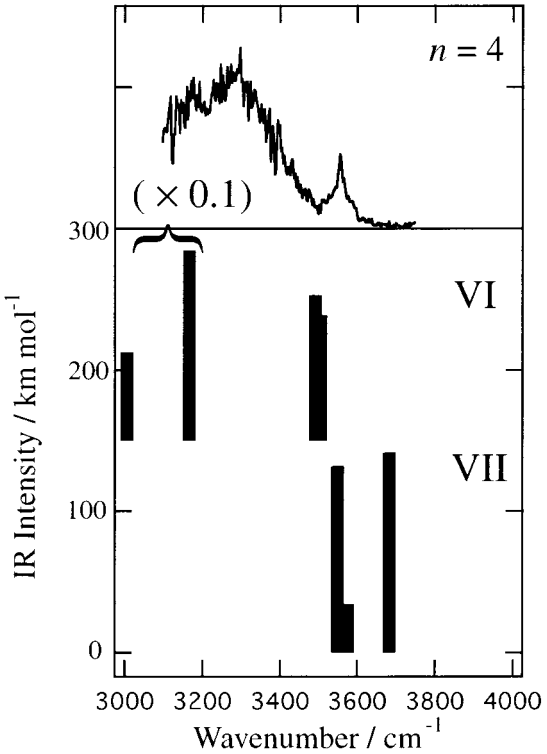

Figure 8. Comparison of the infrared photodissociation spectrum with the calculated infrared spectra for $n = 4$.

attributed mainly to the free OH stretching vibration of $HCOOH_2^+$ and the asymmetric OH stretching vibration of H_2O, respectively. The ion core of the $n = 1$ cluster is $HCOOH_2^+$.

Figure 6 shows the observed and the calculated infrared spectra of $n = 2$. In the observed spectrum, two maxima are seen at 3540 and 3605 cm^{-1}. The calculation for structure II predicts a free OH stretching vibration of HCOOH at 3538 cm^{-1},

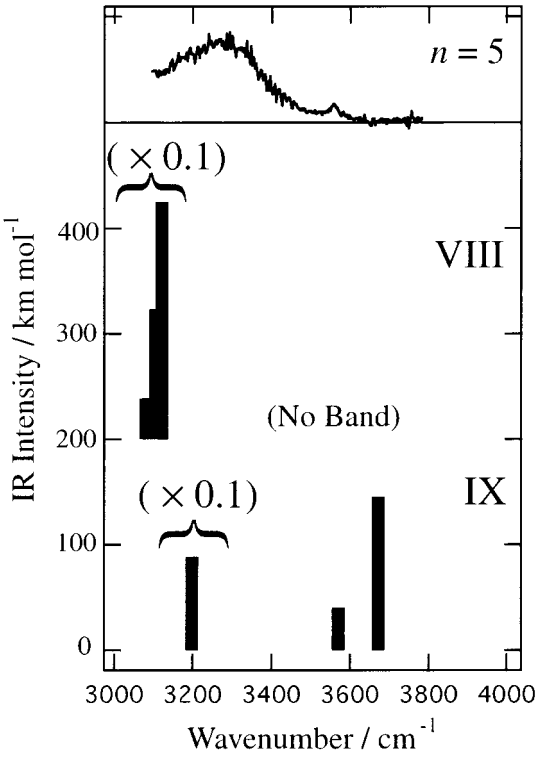

Figure 9. Comparison of the infrared photodissociation spectrum with the calculated infrared spectra for $n = 5$.

TABLE 2: Vibrational Frequencies, Infrared Intensities, and Assignments of the Free OH Stretching Vibrations Obtained by the MO Calculations and the Experiments for $n = 1-3$

n		frequency/ cm^{-1}	intensity/ km mol^{-1}	assignment of free OH
1	I	3442	196	HCOOH
		3539	92	H_2O sym
		3632	225	H_2O asym
	obs[a]	3490		HCOOH
		3570		H_2O asym
2	II	3538	172	HCOOH
		3562	62	H_2O sym
		3663	177	H_2O asym
	III	3478	25	HCOOHasym
		3478	233	HCOOH sym
		3573	192	H_3O^+
	obs[a]	3540		HCOOH
		3605		H_2O asym
3	IV	3487	107	HCOOH
		3568	45	H_2O sym
		3668	153	H_2O asym
	V	3505	92	HCOOH
		3537	165	HCOOH
	obs[a]	3552		HCOOH
		3615		H_2O sym
		3645		H_2O asym

[a] Observed frequencies in the infrared photodissociation spectra.

a symmetric OH stretching vibration of H_2O at 3562 cm^{-1}, and an asymmetric one at 3663 cm^{-1}. For structure III, the calculation provides three bands: a free OH stretching vibration of H_3O^+ at 3573 cm^{-1}, a symmetric OH stretching vibration of two HCOOH molecules at 3478 cm^{-1}, and an asymmetric one at 3478 cm^{-1}. The calculated spectra show that the two lower-frequency bands are relatively close to each other in position for both structures II and III. Therefore, these two bands may appear in the infrared spectrum as overlapping each other. We assign the structure of the $n = 2$ cluster to structure II. Two reasons exist for the assignment; one is that the total energy of

TABLE 3: Vibrational Frequencies, Infrared Intensities, and Assignments of the Free OH Stretching Vibrations Obtained by the MO Calculations and the Experiments for $n = 4$ and 5

n		frequency/ cm^{-1}	intensity/ km mol^{-1}	assignment of free OH
4	VI	3492	103	HCOOH
		3506	89	HCOOH
	VII	3549	132	HCOOH
		3576	34	H_2O sym
		3683	142	H_2O asym
	obs[a]	3555		HCOOH
5	VIII	No band		
	IX	3571	40	H_2O sym
		3672	145	H_2O asym
	obs[a]	No band		

[a] Observed frequencies in the infrared photodissociation spectra.

structure II is lower than that of structure III, and the other is the good coincidence of the observed band position with the calculated one of structure II. The observed band at 3540 cm^{-1} is ascribed to a stack of the two bands: the free OH stretching vibration of HCOOH and the symmetric OH stretching vibration of H_2O. The band at 3605 cm^{-1} is assigned to the asymmetric OH stretching vibration of H_2O. Thus, the ion core of the observed $n = 2$ cluster is attributed to the $HCOOH_2^+$ ion.

The calculated and observed spectra of $n = 3$ are presented in Figure 7. In the observed spectrum, one can see three sharp bands at 3552, 3615, and 3645 cm^{-1} and a broad band around 3200 cm^{-1}. The calculations for structure IV obtain three bands in the 3400−3800 cm^{-1} region: a free OH stretching vibration of HCOOH at 3487 cm^{-1}, a symmetric OH stretching vibration of H_2O at 3568 cm^{-1}, and an asymmetric one at 3668 cm^{-1}. For structure V, the calculation provides two free OH stretching vibrations at 3505 and 3537 cm^{-1}; these vibrations correspond to each of the two HCOOH molecules. These calculated spectra show that the existence of the three bands observed in the 3400−3800 cm^{-1} region is reasonably explained only by structure IV. Therefore, the bands observed at 3552, 3615, and 3645 cm^{-1} could be assigned to the bands at 3487, 3568, and 3668 cm^{-1} in the calculated spectrum of structure IV. There are two discordant features between the observed spectrum and the calculated one of structure IV; the intensity of the observed 3552 cm^{-1} band is about four times as high as that of the 3645 cm^{-1} band, although the calculation for structure IV predicts that the intensity of the former band is lower than that of the latter one, and the calculation provides no band around 3200 cm^{-1} for structure IV. One can solve these contradictions by introducing another isomer: structure V. In the calculated spectrum of structure V, there are two free OH stretching bands of two HCOOH molecules at 3505 and 3537 cm^{-1} and two hydrogen-bonded OH stretching bands at 3215 and 3271 cm^{-1}. The structure V isomer may show some bands around 3200 and 3500 cm^{-1}. The observed spectrum is reasonably explained by the coexistence of the two spectra of structures IV and V. The observed 3552 cm^{-1} band is assigned to the free OH stretching vibrations of HCOOH in both structures IV and V. The 3615 and 3645 cm^{-1} bands correspond to the OH stretching vibrations of H_2O in structure IV. The broad band around 3200 cm^{-1} is attributed to the hydrogen-bonded OH stretching vibrations of structure V. As suggested in the next paragraph, the $n = 4$ cluster has an H_3O^+ ion core. Because the cluster size of $n = 3$ is the critical number of the ion core switch from $HCOOH_2^+$ to H_3O^+, it is probable that there exist two isomers of structures IV and V in our experiments. On the basis of the total energies obtained by the calculations, the major isomer of the $n = 3$ cluster is attributed to structure IV. Thus, one can say that the ion core of the $n = 3$ cluster is the $HCOOH_2^+$.

Figure 8 shows the observed and the calculated infrared spectra of $n = 4$. A sharp band at 3555 cm^{-1} and a rather broader band around 3300 cm^{-1} are seen in the observed spectrum. No band is observed in the 3600−3800 cm^{-1} region. In the calculated spectrum of structure VI, the two free OH stretching vibrations of the two HCOOH molecules appear at 3492 and 3506 cm^{-1}. Two hydrogen-bonded OH stretching vibrations also exist at 3005 and 3167 cm^{-1}. On the other hand, structure VII has three bands in the 3400−3800 cm^{-1} region: a free OH stretching vibration of HCOOH at 3549 cm^{-1}, a symmetric OH stretching vibration of H_2O at 3576 cm^{-1}, and an asymmetric one at 3683 cm^{-1}. Apparently, the calculated spectrum of structure VI agrees very well with the observed one; the observed 3555 cm^{-1} band is assigned to the free OH stretching bands of structure VI, and the broad band around 3300 cm^{-1} is attributed to the hydrogen-bonded OH stretching bands of the same isomer. Consequently, the structure of the $n = 4$ cluster is attributed to structure VI, and the ion core is the H_3O^+ ion. This result suggests that the clusters switch the ion cores from $HCOOH_2^+$ for $n = 1-3$ to H_3O^+ for $n = 4$.

The calculated and the observed spectra of $n = 5$ are presented in Figure 9. In the observed spectrum, a very broad band is observed at 3300 cm^{-1}. There is also a very weak band at about 3550 cm^{-1}. For $n = 5$, the calculation predicts the existence of an isomer with a free COH group with a total energy higher than that of structure VIII by 2722 cm^{-1}. This isomer has a structure similar to structure VI with a cyclic dimer instead of the end molecule. This minor band is thought to be due to this isomer. The calculated spectrum of structure VIII predicts a few hydrogen-bonded OH stretching vibrations around 3100 cm^{-1}; no band is obtained in the 3500−3800 cm^{-1} region. For structure IX, two OH stretching vibrations of H_2O exist at 3571 and 3672 cm^{-1}, in addition to a hydrogen-bonded OH stretching vibration at 3198 cm^{-1}. The spectral features of the observed spectrum resemble those of the calculated spectrum of structure VIII; the strong bands appear in the 3000−3500 cm^{-1} region, and no strong band emerges in the 3500−3800 cm^{-1} region. We conclude that the $n = 5$ cluster has the cyclic structure like structure VIII and that the ion core is the H_3O^+ ion. For structure VIII, the H_3O^+ ion core is located in the central position of a ring. The ring consists of all of the five formic acid molecules. Each formic acid molecule is bound to the neighbors by the OH···O═C hydrogen bonds. The MO calculations predict a similar structural isomer also for the $n = 4$ cluster; the isomer has an H_3O^+ ion core and a four-member ring. In this case, however, the isomer is less stable than structure VI by 164 cm^{-1}. Therefore, the five-member ring is the most suitable for surrounding and stabilizing the H_3O^+ ion core. This structural advantage must be the main reason for the magic number of $n = 5$.

5. Conclusions

Infrared photodissociation spectroscopy and ab initio MO calculations were applied to the structural analysis of $H^+ \cdot (HCOOH)_n \cdot H_2O$ with $n = 1-5$. The MO calculations predict that the ion core switch may occur from $HCOOH_2^+$ to H_3O^+ between $n = 3$ and 4. We confirm this result by comparing the observed infrared spectra with the calculated ones. The calculated spectra of the most stable isomers reasonably agree with the observed ones. For $n = 1-3$, the asymmetric OH stretching band of H_2O emerges in the spectra. For $n = 4$ and 5, on the other hand, it disappears in the spectra. These spectral features

suggest that the H_2O molecule is at the periphery of the clusters for $n = 1-3$ and that it is in the inside position of the clusters existing as H_3O^+ for $n = 4$ and 5. The ion core switch occurs from $HCOOH_2^+$ for $n = 1-3$ to H_3O^+ for $n = 4$ and 5 in the $H^+ \cdot (HCOOH)_n \cdot H_2O$ clusters. It is spectroscopically confirmed that the $n = 5$ cluster has a particularly stable, cyclic-type structure.

References and Notes

(1) Yeh, L. I.; Okumura, M.; Myers, J. D.; Price, J. M.; Lee, Y. T. *J. Chem. Phys.* **1989**, *91*, 7319.
(2) Bieske, E. J.; Maier, J. P. *Chem. Rev.* **1993**, *93*, 2603.
(3) Lisy, J. M. *Cluster Ions*; Wiley: Chichester, U.K., 1993; p 217.
(4) Ohashi, K.; Izutsu, H.; Inokuchi, Y.; Hino, K.; Nishi, N.; Sekiya, H. *Chem. Phys. Lett.* **2000**, *321*, 406.
(5) Ohashi, K.; Inokuchi, Y.; Izutsu, H.; Hino, K.; Yamamoto, N.; Nishi, N.; Sekiya, H. *Chem. Phys. Lett.* **2000**, *323*, 43.
(6) Nishi, N.; Nakabayashi, T.; Kosugi, K. *J. Phys. Chem. A* **1999**, *103*, 10851.
(7) Leiserowitz, L. *Acta Crystallogr.* **1976**, *B32*, 775.
(8) Karle, J.; Brockway, L. O. *J. Am. Chem. Soc.* **1944**, *66*, 574.
(9) Feng, W. Y.; Lifshitz, C. *J. Phys. Chem.* **1994**, *98*, 6075.
(10) Zhang, R.; Lifshitz, C. *J. Phys. Chem.* **1996**, *100*, 960.
(11) Aviyente, V.; Zhang, R.; Varnali, T.; Lifshitz, C. *Int. J. Mass Spectrom. Ion Processes* **1997**, *161*, 123.
(12) Kosugi, K.; Inokuchi, Y.; Nishi, N. *J. Chem. Phys.* **2001**, *114*, 4805.
(13) Inokuchi, Y.; Nishi, N. *J. Chem. Phys.* **2001**, *114*, 7059.
(14) Frisch, M. J.; Trucks, G. W.; Schlegel, H. B.; Scuseria, G. E.; Robb, M. A.; Cheeseman, J. R.; Zakrzewski, V. G.; Montgomery, J. A., Jr.; Stratmann, R. E.; Burant, J. C.; Dapprich, S.; Millam, J. M.; Daniels, A. D.; Kudin, K. N.; Strain, M. C.; Farkas, O.; Tomasi, J.; Barone, V.; Cossi, M.; Cammi, R.; Mennucci, B.; Pomelli, C.; Adamo, C.; Clifford, S.; Ochterski, J.; Petersson, G. A.; Ayala, P. Y.; Cui, Q.; Morokuma, K.; Malick, D. K.; Rabuck, A. D.; Raghavachari, K.; Foresman, J. B.; Cioslowski, J.; Ortiz, J. V.; Stefanov, B. B.; Liu, G.; Liashenko, A.; Piskorz, P.; Komaromi, I.; Gomperts, R.; Martin, R. L.; Fox, D. J.; Keith, T.; Al-Laham, M. A.; Peng, C. Y.; Nanayakkara, A.; Gonzalez, C.; Challacombe, M.; Gill, P. M. W.; Johnson, B. G.; Chen, W.; Wong, M. W.; Andres, J. L.; Head-Gordon, M.; Replogle, E. S.; Pople, J. A. *Gaussian 98*, revision A.9; Gaussian, Inc.: Pittsburgh, PA, 1998.
(15) Hunter, E. P.; Lias, S. G. *J. Phys. Chem. Ref. Data* **1998**, *27*, 413.
(16) Pettersson, M.; Lundell, J.; Khriachtchev, L.; Räsänen, M. *J. Am. Chem. Soc.* **1997**, *119*, 11715.
(17) Herzberg, G. *Molecular Spectra and Molecular Structure II*; Krieger: Malabar, FL, 1991; Chapter 3.